The construction of a lymphoma cell-based, DC-targeted vaccine, and its application in lymphoma prevention and cure

Tianlin Zhou[a], Jinrong Peng[a], Ying Hao[a], Kun Shi[a], Kai Zhou[a], Yun Yang[a], Chengli Yang[a], Xinlong He[a], Xinmian Chen[b], Zhiyong Qian[a],*

[a] State Key Laboratory of Biotherapy and Cancer Center, West China Hospital, Sichuan University, and Collaborative Innovation Center of Biotherapy, Chengdu, 610041, PR China
[b] Personalized Drug Therapy Key Laboratory of Sichuan Province, Department of pharmacy, Sichuan Provincial People's Hospital, School of Medicine, University of Electronic Science and Technology of China, Chengdu, 610072, PR China

A R T I C L E   I N F O

A B S T R A C T

In recent years, Non-Hodgkin lymphoma (NHL) has been one of the most fast-growing malignant tumor diseases. NHL poses severe damages to physical health and a heavy burden to patients. Traditional therapies (chemotherapy or radiotherapy) bring some benefit to patients, but have severe adverse effects and do not prevent relapse. The relevance of emerging immunotherapy options (immune-checkpoint blockers or adoptive cellular methods) for NHL remains uncertain, and more intensive evaluations are needed. In this work, inspired by the idea of vaccination to promote an immune response to destroy tumors, we used a biomaterial-based strategy to improve a tumor cell-based vaccine and constructed a novel vaccine named Man-EG7/CH@CpG with antitumor properties. In this vaccine, natural tumor cells are used as a vector to load CpG-ODN, and following lethal irradiation, the formulations were decorated with mannose. The study of the characterization of the double-improved vaccine evidenced the enhanced ability of DCs targeting and improved immunocompetence, which displayed an antitumor function.

In the lymphoma prevention model, the Man-EG7/CH@CpG vaccine restrained tumor formation with high efficiency. Furthermore, unlike the non-improved vaccine, the double-improved vaccine elicited an enhanced antitumor effect in the lymphoma treatment model. Next, to improve the moderate therapeutic effect of the mono-treatment method, we incorporated a chemotherapeutic drug (doxorubicin, DOX) into the process of vaccination and devised a combination regimen. Fortunately, a tumor inhibition rate of ~85% was achieved via the combination therapy, which could not be achieved by mono-chemotherapy or mono-immunotherapy. In summary, the strategy presented here may provide a novel direction in the establishment of a tumor vaccine and is the basis for a prioritization scheme of immuno-chemotherapy in enhancing the therapeutic effect on NHL.

1. Introduction

Non-Hodgkin lymphoma (NHL) is a kind of malignant tumor disease that originates in the lymphoid and hematopoietic system. In recent years, due to an increasingly aging population and changes in people's lifestyle, the morbidity and mortality of NHL have increased promptly [1,2]. According to statistics, the NHL is one of the ten leading cancer types, which globally caused more than 488,000 new cancer cases and 249,000 deaths in 2017. The incidence of NHL has increased by 39% since 2007, and younger people are starting to be affected, making NHL a significant threat to the public health and social development [3,4]. It has been traditionally treated by chemotherapy or radiotherapy [5].

However, the side effects caused by these methods, which brings additional trouble to patients. Meanwhile, challenges of drug resistance, relapse, and others compromise to a large extent the NHL therapy [6–9]. Thus, new solutions are urgently required.

Cancer immunotherapy, which harnesses the delicate specificity of the immune system to destroy tumors, has been attempted and developed for more than a century [10–13]. Following the development of oncology and immunology as sciences, the complexity of immune therapeutics in the immune system is exemplified by the myriad of ongoing investigations taking place in parallel [14]. Some immune therapeutics have been approved by the FDA and were successfully used in the clinic [15,16]. The representative immuno-therapeutic drug

---

of NHL is rituximab, which targets the marker of CD20 of lymphoma cells. The rituximab plus CHOP (a chemotherapy program) combination (R–CHOP) regimen indeed improved long-term outcomes of patients and has been used as the first-line treatment for many patients [16]. However, problems associated with chemotherapeutic drugs remain, namely the poor targeting capability and severe side effects, which result in a modest curative effect and harmful organism adaptation. ICBs (Immune-Checkpoint Blockers) has recently emerged, and also utilized to treat NHL patients. Still, its efficacy should be further evaluated [17]. Adoptive cellular therapy (ACT) is another immunotherapy strategy [18]. For certain NHLs, ACT-based therapies are available for precise targeting in several individuals. However, the severe adverse effects due to cytokine release syndrome (CRS) or others restricts the application of these therapies [19]. Given the shortcomings of traditional and emerging treatment options, improved methods are urgently needed to tackle NHL.

In contrast to the above strategies, tumor vaccines, which are designed to expand tumor-specific T-cell responses through enhanced active immunization, have long been anticipated as probable effective cancer immunotherapy [20,21]. The antigen categories of the tumor vaccines are varied [22,23], among which, whole tumor cell-based vaccines have been employed in numerous studies over the past decade, which can offer several advantages over subunit and peptide vaccines [24,25], and hundreds of them were tested in clinical trials to date [26–28]. Repeated freeze-thaw and irradiation methods are commonly used to prepare whole tumor cell vaccines [29]. In particular, the irradiation method, which can induce immunogenic cell death (ICD) to produce numerous antigens to activate the antitumor effect, is widely adopted [30]. Although the polyclonal immune response with the expansion of individual antigen-specific T cells is primed via tumor cell vaccines, most of the responses elicited by a mixture of self-antigens and non-self-antigens may not reach the threshold for the number of anticancer T cells needed, and adversely side effects may appear after the administrations [31]. Optimizations have been tried, such as genetically modifying tumor cells to produce cytokines (GM-CSF, TGF-β, and so on), which enhanced the stimulation of antitumor response or relieved the immunosuppressive effect [32,33]. In addition, biomaterials with good biocompatibility have been recently developed to delivery therapeutics [34–40], which can be flexibly designed to meet the modification needs of vaccines to enhance antitumor immune activity [41–43]. Unfortunately, these optimizations cannot solve the existing challenges substantially, and multi-treatments provide new directions of lymphomas' therapy potentially. Traditional tumor cell vaccines have a low DC-targeting effect, which generates a weak immune response and poor tumor-resist effect [44]. Therefore, the antigen immunogenicity of tumor cell vaccine, and the function of a DC-targeting vaccine should be improved.

Hence, in this work, CpG compounding, DC targeting by a double-improved vaccine, and a chemotherapeutic agent combination system was established by modifying the tumor cells to improve their immunocompetence using chemotherapeutics, thus uniting immunotherapy and chemotherapy against lymphoma (Scheme 1). First, we have condensed the CpG-ODN adjuvant via chitosan, which is derived from chitin and was approved by the FDA to deliver antigens or adjuvants [45,46]. Furthermore, we prepared formulations by introducing a chitosan-coated CpG complex (CH@CpG) to EG7 cells. CpG-ODN is ubiquitous in the bacterial genome but is not present in the invertebrate genome. It can prompt the body to produce a defense effect and activate the immune response, making it an ideal adjuvant [47,48]. Efficient antigen delivery to DCs is a prerequisite for an antitumor immune response [44]. Avrameas et al. found that many lectin-like receptors exist on the surface of DCs, which can phagocytize mannose effectively via a binding reaction [49,50]. Next, after lethal irradiation to ease the EG7/CH@CpG formulation, the formulation was further modified with DSPE-PEG-Mannose ligand to targeting DCs [51,52]. Eventually, a double-improved vaccine of Man-EG7/CH@CpG was

constructed and shown to have improved immunocompetence and enhanced targeting effect. The vaccine of Man-EG7/CH@CpG effectively inhibited tumor formation in the lymphoma prevention model and decreased tumor growth in the lymphoma treatment model compared with traditional tumor cell vaccines. Furthermore, numerous studies have indicated that it is challenging for a mono-treatment to achieve the antitumor effect threshold [53,54]. Although side effects existed, chemotherapeutic drugs (e.g. doxorubicin) are still widely applied in multi-subtypes of lymphoma in clinical settings, which can inhibit tumor growth to some extend [2]. Therefore, based on the treatment of a murine lymphoma model with the Man-EG7/CH@CpG vaccine, we added a chemotherapy drug (doxorubicin, DOX). We developed a combined regimen, expecting to destroy tumors as efficiently as possible. A synergistic therapeutic effect was observed that significantly boosted tumor suppression compared with mono-chemotherapy or mono-immunotherapy. Our work offered a simple immunotherapy and chemotherapy combined strategy to enhance the immunocompetence of vaccines by targeting modified and adjuvant compounds and improve the little relief of chemotherapy via a synergistic multi-therapeutic effect. This work lays the foundation for the design of potential novel strategies to expand the curative effect of immuno-chemotherapy to NHL.

2. Materials and methods

2.1. Materials

Chitosan was purchased from Sigma-Aldrich (catalog:448869,50000–190000Da,75–85% deacetylation, Saint Louis, USA). CpG-ODN (phosphorothioate modified, TCCATGACGTTCCTGAC GTT) and doxorubicin hydrochloride (DOX) were purchased from Sangon Biotech (Shanghai) Co., Ltd. DSPE-PEG-FITC and DSPE-PEG-Mannose were purchased from Xian ruixi Biological Technology Co., Ltd. Roswell Park Memorial Institute medium (RPMI-1640), Dulbecco's modified Eagle's medium (DMEM), penicillin-streptomycin liquid (100X), and fetal bovine serum (FBS) were purchased from HyClone (Logan, USA). Murine GM-CSF was purchased from peprotech (USA). PrimeScript™ RT reagent Kit was purchased from TaKaRa (Japan). iTaq™ Universal SYBR® Green Supermix was purchased from BIO-RAD (USA). CFDA SE Cell Proliferation Assay and Tracking Kit was purchased from Beyotime (Shanghai). F4/80-FITC monoclonal antibody (catalog:123107, clone:BM8) and CD3-PE monoclonal antibody (catalog:100205, clone:17A2) were purchased from BioLegend (USA). CD3-FITC monoclonal antibody (catalog:555274,clone:17A2), CD4-APC monoclonal antibody (catalog:553051,clone:RM4-5), CD8a-APC monoclonal antibody (catalog:553053,clone:53–6.7), Foxp3-PE monoclonal antibody (catalog:563101,clone:R16-715), IFNγ-PE monoclonal antibody (catalog:554412,clone:XMG1.2), CD11c-FITC monoclonal antibody (catalog:553801,clone:HL3), CD80-PE monoclonal antibody (catalog:553769,clone:16-10A1) and CD86-APC monoclonal antibody (catalog:558703,clone:GL1) monoclonal antibody for flow cytometry and immunofluorescence were all purchased from BD Biosciences (USA).

2.2. Cell culture

EG7-OVA cells were originally obtained from American Type Culture Collection (Rockville, MD) and were respectively cultured in RPMI-1640 and DMEM media containing 10% FBS, penicillin (100 U/mL), and streptomycin (100 mg/mL). The cell cultures were maintained in an incubator at 37 °C with a humidified 5% CO2 atmosphere.

2.3. Animals

Six to eight weeks old female C57BL/6 mice were purchased from HFK Bioscience Co., Ltd. (Beijing, China) and kept under specific
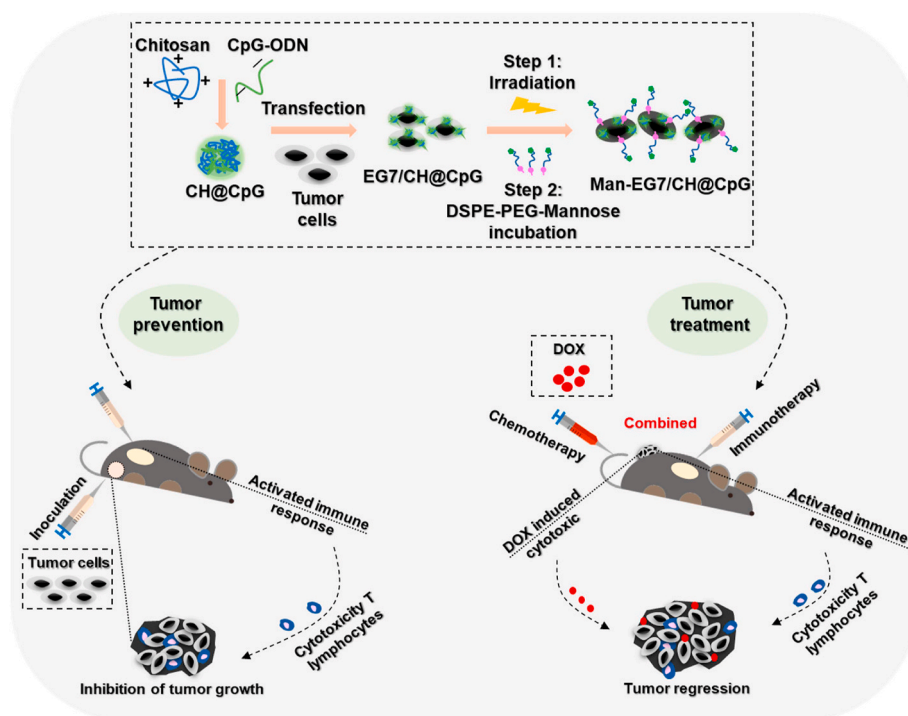
Scheme 1. Schematic view of Man-EG7/CH@CpG vaccine combination with DOX drugs in lymphoma therapy.

pathogen free (SPF) condition with free access to standard food and water. All animal procedures were performed following the protocols approved by the Institutional Animal Care and Treatment Committee of Sichuan University (Chengdu, P. R. China).

2.4. Preparation of man-EG7/CH@CpG vaccine

The CpG-ODN binding ability of chitosan was evaluated by agarose-retarding assay: 1 μg of CpG-ODN was separately mixed with different mass ratios (chitosan: CpG-ODN = 0.5:1, 1:1, 2:1, 4:1, 5:1, 8:1) of chitosan. Electrophoresis was then performed on a 1% (w/v) agarose gel for 15 min at 120 V, which was stained with Gelred. Gels were visualized and imaged using ChemiDoc Imagers.

EG7-OVA cells were seeded into a 6-well plate at a density of 1×10^6 cells per well 24 h before transfection. CY5 labeled CpG-ODN (CpG-ODN^{CY5}, Sangon Biotech, Shanghai) was purchased as a visualized reporter to test the uptake efficiency. The mass ratio of chitosan and CpG-ODN(4 μg/mL) to 5:1 was incubated in RPMI-1640 medium (serum-free) for 15–30 min at normal temperature, then sprinkled into the cultured tumor cells. DOTAP/CpG (5:1, mass ratio) or Lipo3K/CpG (5:1, mass ratio) complex with an equal amount of CpG-ODN was used as control. Pictures of each well were taken under a microscope, and the transfection efficiency was determined by flow cytometry after 12 h (NovoCyte Flow Cytometer, ACEA Biosciences, USA). The EG7/Chitosan/CpG complex was inactivated at lethally irradiated (150 Gy) conditions using an RS-2000 irradiation equipment (Rad Source Technologies, USA). Next, DSPE-PEG-Mannose(50 μg/ml) was mixed with the inactivated modification tumor cells, which were absorbed with adjuvant for 24 h at 37 temperature. This prepared formulation was labeled as Man-EG7/CH@CpG.

2.5. BMDC's uptake of man-EG7/CH@CpG vaccine in vitro

FITC labeled CpG-ODN (CpG-ODN^{FITC}, Sangon Biotech, Shanghai) was purchased to establish a vaccine to test the uptake efficiency. The induction method of bone marrow-derived dendritic cells (BMDCs) was described in a previous study [55]. After the process of BMDC induction, these cells were used for the next experiment directly. BMDCs were seeded in 24-well plates at a density of 1×10^5 cells per well 24 h before uptake. For uptake experiments, the prepared Man-EG7/CH@CpG^{FITC} (1×10^5) was added to the cultured BMDCs. BMDCs mixed with an equal amount of EG7/CH@CpG^{FITC} were used as controls. 24 Hours later, pictures of wells were taken under a microscope, and the uptake efficiency was further detected using flow cytometry (NovoCyte Flow Cytometer, ACEA Biosciences, USA).

2.6. Mature assay of BMDCs after vaccine stimulations

The induced BMDCs were seeded into a 6-well plate at a density of 5×10^5 cells per well 24 h before stimulation. Then, the Man-EG7/CH@CpG (5×10^5) was added. Simultaneously, CpG, CH@CpG, EG7, and EG7/CH@CpG (containing the same amount of CpG or cells) were separately added and used as controls. 24 h post-stimulation, BMDCs were collected and co-stained with FITC-conjugated CD11c, PE-conjugated CD80, and APC-conjugated CD86 antibodies for 30 min at 4 °C and then analyzed by flow cytometry (NovoCyte Flow Cytometer, ACEA Biosciences, USA).

2.7. Activation assays of BMDCs after vaccine stimulation

Cytokine secretion patterns reflect the activation BMDCs, and qPCR (Quantitative Real-time PCR) was employed to measure the mRNA expression level of cytokines in BMDCs. In this study, BMDCs were first seeded into a 6-well plate at a density of 1×10^6 cells per well 24 h before stimulation. The Man-EG7/CH@CpG (1×10^6) was added to wells. Equal amounts of EG7/CH@CpG were added into the corresponding wells and acted as controls. BMDCs were harvested after 24 h, and RNA was isolated and reverse transcribed to cDNA by a PrimeScript™ RT reagent kit (Takara, Japan). Next, qPCR amplification for related primers was performed using iTaqTM Universal SYBR@ Green Supermix (Bio-Rad) and CFX96 Real-Time PCR Detection System (Bio-Rad). All primers are shown in Supplementary Table 1.

2.8. Targeting assay of the vaccine in vivo

CY5 labeled CpG-ODN (CpG-ODN, Sangon Biotech, Shanghai) was used to produce Man-EG7/CH@CpG and EG7/CH@CpG. C57BL/6 mice were subcutaneously injected with Man-EG7/CH@CpG (2×10^6) or EG7/CH@CpG (2×10^6). Mice without immunization were used as controls. Mice were sacrificed to detect the targeting efficiency at different time points (3 h and 6 h). In lymph node uptake detection, lymph nodes from the subcutaneous model were minced into small pieces to release immune cells; the obtained cells were next analyzed by flow cytometry. For DCs or macrophage uptake detection, the collected immune cells were first stained with FITC-conjugated CD11c or FITC-conjugated F4/80 antibody for 30 min at 4 °C, then analyzed by flow cytometry (NovoCyte Flow Cytometer, ACEA Biosciences, USA).

2.9. Activation assays of the vaccine in vivo

For the detection of the vaccine in vivo, female C57BL/6 mice (6–8 weeks old) were subcutaneously injected with EG7, EG7/CH@CpG, Man-EG7/CH@CpG, and CH@CpG (on days 0, 7, and 14), and the vaccine of each group contained equal amount of CpG(4 μg/mL) or cells (2×10^6). Mice injected with PBS were used as controls (NS group, four mice per group). One week after the third injection, murine spleen lymphocytes in each group were isolated and marked by CFSE for 30 min at 37 °C. After that, lymphocytes in the different groups were seeded in a 96-well plate at a density of 1×10^5 cells per well and then stimulated by lethally irradiated EG7 cells (1×10^5) for four days. Lymphocytes without any stimulation were used as controls. Eventually, lymphocytes were collected in tubes, stained with PE-conjugated CD3 antibody, and measured by flow cytometry (NovoCyte Flow Cytometer, ACEA Biosciences, USA).

2.10. Antitumor performance in vivo

In the tumor-prevention model, female C57BL/6 mice (6–8 weeks old) were first injected with a different vaccine, which was mentioned in the assay of biological activation above. One week after the last injection, high survival EG7 cells (1×10^6) were inoculated on the back of mice. 18 Days later, mice were sacrificed, tumors were photographed and weighted, and lymph nodes were also harvested and photographed. The tumor formation situation of each group was measured every day.

For the tumor subcutaneous treatment model, female C57BL/6 mice (6–8 weeks old) were inoculated with 1×10^6 EG7 cells on day 0. On day 3, mice were randomly divided into five groups (4 mice per group) and injected with PBS (NS), CH@CpG, EG7, EG7/CH@CpG, and Man-EG7/CH@CpG for three treatments (seven weeks apart in each injection), which was consistent in the assay of biological activation above. On day 22, all mice were sacrificed, and tumors and immune organs (spleens and lymph nodes) were photographed and weighed. The tumor volume and bodyweight of mice were measured every other day; the relative tumor volume was calculated using the formula: $0.5 \times$ length (mm) $\times$ width^2 (mm^2).

2.11. Evaluation of in vivo tumor growth inhibition of combined therapy strategies

C57BL/6 mice (female, 6–8 weeks old) were first subcutaneously injected with 1×10^6 EG7 on the back. Three days later, the mice were randomly divided into six groups (4 mice per group) and injected with PBS (NS), CH@CpG, EG7, EG7/CH@CpG, or Man-EG7/CH@CpG on the back (one week apart in each injection, three times), which was consistent in the assay of biological activation above. After 4 days of the first immune treatment, DOX (1.5 mg/kg) was intravenously injected into the tail vein (one week apart in each injection, three times). The dosing intervals of which is also widely adopted in previous study [56–59]. Mice treated with DOX only were used as positive controls.

For tumor volume detection, tumors were measured every other day, and the relative tumor volume was calculated according to the following formula: $0.5 \times$ length (mm) $\times$ width^2 (mm^2). On day 25, mice were sacrificed, tumors were weighed, and the main organs were collected for further analysis. For the survival model, mice were treated via same administration method, but instead of sacrificing the animals on day 25, they underwent daily observation on 45 days.

2.12. Flow cytometry assay of lymphocytes of immune organs

Lymphocytes of spleens and lymph nodes from the combined therapy mouse model were collected separately, with FITC-CD3, APC-CD8, and PE-IFNγ antibodies to detect the number of cytotoxic T cells, and co-stained with FITC-CD3, APC-CD4, and PE-Foxp3 antibodies to identify the number of Tregs cells via flow cytometry (NovoCyte Flow Cytometer, ACEA Biosciences, USA).

2.13. Histological analysis

Tumor tissue and main organs were harvested from in vivo experiments and embedded in paraffin. For the assay of tumor immune infiltration, tumor sections were prepared, blocked, and subsequently incubated with FITC-CD3 and PE-CD8 antibodies at 4 °C for 30 min. 4′,6-diamidino-2-phenylindole (DAPI) was stained next for 10 min at room temperature as the nuclear counterstain. The fluorescent image was visualized and captured by a fluorescence microscope (Olympus, Japan). Besides, the main organ tissue sections were subjected to hematoxylin-eosin (HE) staining to detect the toxicity of the combined therapy.

2.14. Statistical analysis

Data were expressed as means with 95% confidence intervals. Statistical analysis was performed using a two-tailed Student's t-test or one-way analysis of variance (ANOVA) using Prism 5.0c Software (GraphPad Software, La Jolla, CA). For all results, a statistically significant difference was defined by a value of * P < 0.05, **P < 0.01, ***P < 0.001.

3. Results

3.1. Fabrication of tumor cell-based double-improved man-EG7/CH@CpG vaccine

In our study, chitosan was used to load and deliver CpG-ODN (Fig. 1A, up). To evaluate the combination ability of chitosan with CpG-ODN, a gel-retarding assay was performed. As shown in Fig. 1B, when the mass ratio of chitosan: CpG-ODN was 5:1, no bright nucleotide band could be observed, suggesting that the CpG-ODN nucleotide was completely loaded by chitosan through an interacting effect and formed a CH@CpG complex. Besides, the transfection status of tumor cells was also shown to be efficient (Supplementary Fig. 1). This ratio (chitosan: CpG-ODN = 5:1) was therefore chosen for the following application in our study. We further optimized the concentration of CpG-ODN, and detected the transfection effciency with DOTAP or Lipo3K in vitro (Supplementary Fig. 2). According to our results, the delivery efficiency of CpG-ODN to tumor cells can be up to 90% under CpG = 4 μg/mL condition with chitosan loaded. The devised cell-adjuvant complex (EG7/CH@CpG) was next lethally irradiated (Fig. 1A, middle) and decorated with mannose (Fig. 1A, down). We detected the situation of lethally irradiated EG7/CH@CpG formulations (Supplementary Fig. 3) and optimized the concentration of DSPE-PEG-Mannose (Supplementary Fig. 4, 50 μg/mL). The assay of colocalization was chosen to verify the CH@CpG uptake and efficiency of the ligand decoration of tumor cells. To track these processes, CY5-conjugated CpG-ODN and DSPE-PEG-FITC were used. According to our results, at
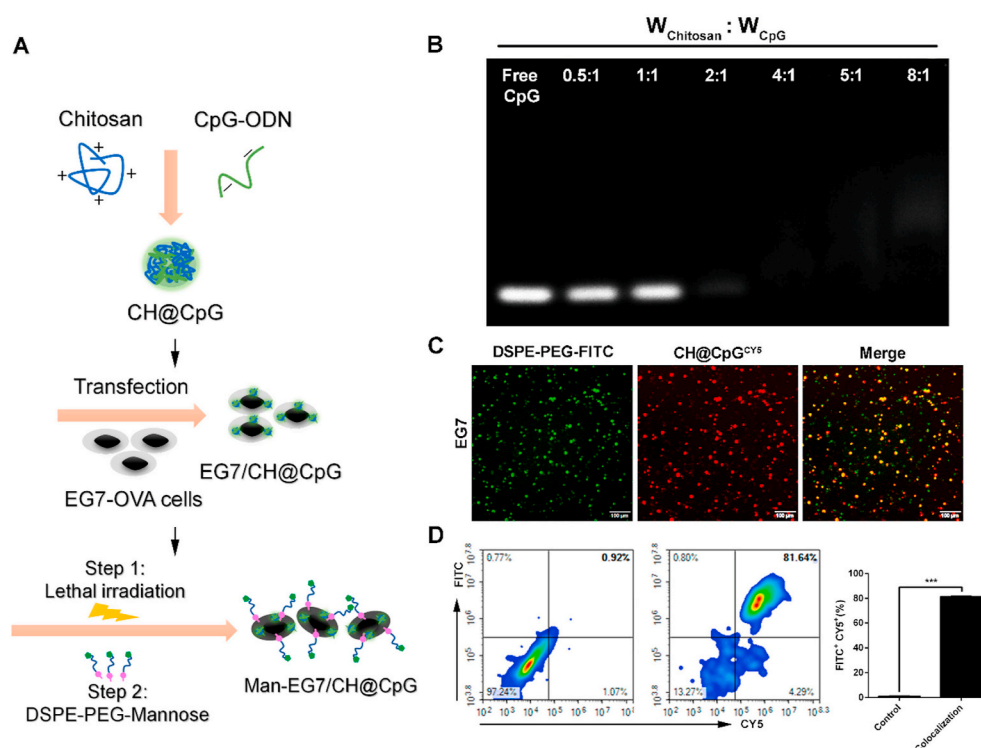
24 h post-dual-ameliorating decoration, significant green-red fluorescence was observed in fluorescent images (Fig. 1C), and colocalization efficiencies of > 80% were detected further (Fig. 1D). It is worth noting that lethal irradiation by X rays (RS-2000) was added for inactivation after the CH@CpG was absorbed into tumor cells.

3.2. Uptake characterization of man-EG7/CH@CpG vaccine by BMDCs

Next, we tested the uptake efficiency after targeting ligand decoration of EG7/CH@CpG formulation. We first extracted and induced primary BMDCs mixed with or without mannose-binding (FITC labeled CpG-ODN) formulations and then detected the uptake characterization of them. The results of all EG7/CH@CpG contained formulations, Man-EG7/CH@CpG formulations showed the best absorption into BMDCs on the whole; some BMDCs were even able to ingest multi-formulations when the EG7/CH@CpG was decorated with mannose (Fig. 2B). The Man-EG7/CH@CpG uptake by BMDC efficiency was > 75%, which is almost 10% Points more than the uptake efficiency of EG7/CH@CpG (Fig. 2C and D), and a significant increase in mean fluorescence intensity (MFI) of Man-EG7/CH@CpG was also observed (P < 0.001) (Fig. 2E). These data indicate that the mannose binding to EG7/CH@CpG formulations improves the targeting of APCs (Fig. 2A).

3.3. Man-EG7/CH@CpG vaccine promotes BMDC's maturation and increases cytokine secreting in vitro

We used the vaccine that involves CpG-ODN (TLR9 ligand), DSPE-PEG-Mannose (APCs targeting ligand), and lethally irradiated EG7 (tumor-specific antigens) to activate BMDCs, which may generate tumor-specific cytotoxicity killing via multiple pathways. According to our results, Man-EG7/CH@CpG indeed increased the abundance of CD11c$^+$CD80$^+$CD86$^+$ DCs (matured DCs), when compared with other formulations (Fig. 3A), and the matured population rate of stimulated DCs reached 55%, which was nearly 30% Points higher than stimulation before (Fig. 3B). The function of DCs mainly depends on the secreting of cytokines [60]. Next, we tested whether EG7/CH@CpG or Man-EG7/CH@CpG formulations could stimulate DCs to produce

cytokines. In our qPCR results (Fig. 3C–F), the test groups significantly increased the mRNA expression levels of TNFα, IFNα4, IFNβ, and IFNγ, which were at least tenfold higher than those in the unstimulated groups (P < 0.05). Compared with the vaccine without mannose binding, the mRNA expression levels of IFNα, IFNβ, IFNγ, and TNFα in the Man-EG7/CH@CpG stimulation group were higher. However, no significant difference was found between the two groups. Our results indicate that the double-improved vaccine efficiently promotes the maturation of DCs and stimulates the secretion of cytokines of DCs, which may activate the immune response to inhibit the growth of tumor cells in vivo.

3.4. In vivo APC targeting of man-EG7/CH@CpG vaccine

To investigate the APC targeting effect, Man-EG7/CH@CpG was administered by subcutaneous injection at the back site of mice. We selected the injection site because it is also the preferred injection route in the tumor treatment model that we will later use. For convenient detection, CpG-ODN was labeled with CY5 fluorochrome. The results showed the lymph node targeting fluorescence uptake signals corresponding to EG7/CH@CpG and Man-EG7/CH@CpG treatment groups at designated time points in which the rate of CY5 positive cells of the Man-EG7/CH@CpG vaccine group was nearly twofold higher than that in the EG7/CH@CpG vaccine group (Fig. 4A and B). The MFI was also quantified and is presented in Fig. 4C; the intensity of mean fluorescence was significantly increased in the Man-EG7/CH@CpG vaccine group.

Lymph nodes are an essential immune organ of the body; it is necessary that the antigen-presenting cells in lymph nodes uptake and process antigens efficiently for initiating an immune response to tumor cells [61,62]. Therefore, the detached cells were stained with fluorescent-tagged CD11c or F4/80 antibody and analyzed further. In contrast to the non-improved vaccine group, a robust uptake rate was detected in DCs (Fig. 4D), and a higher accumulation rate in macrophages was observed at 3 h or 6 h after injection (Fig. 4E). The uptake rate of the EG7/CH@CpG vaccine by APCs was just about half that of the Man-EG7/CH@CpG vaccine. Mannose is the active ligand of lectin receptors
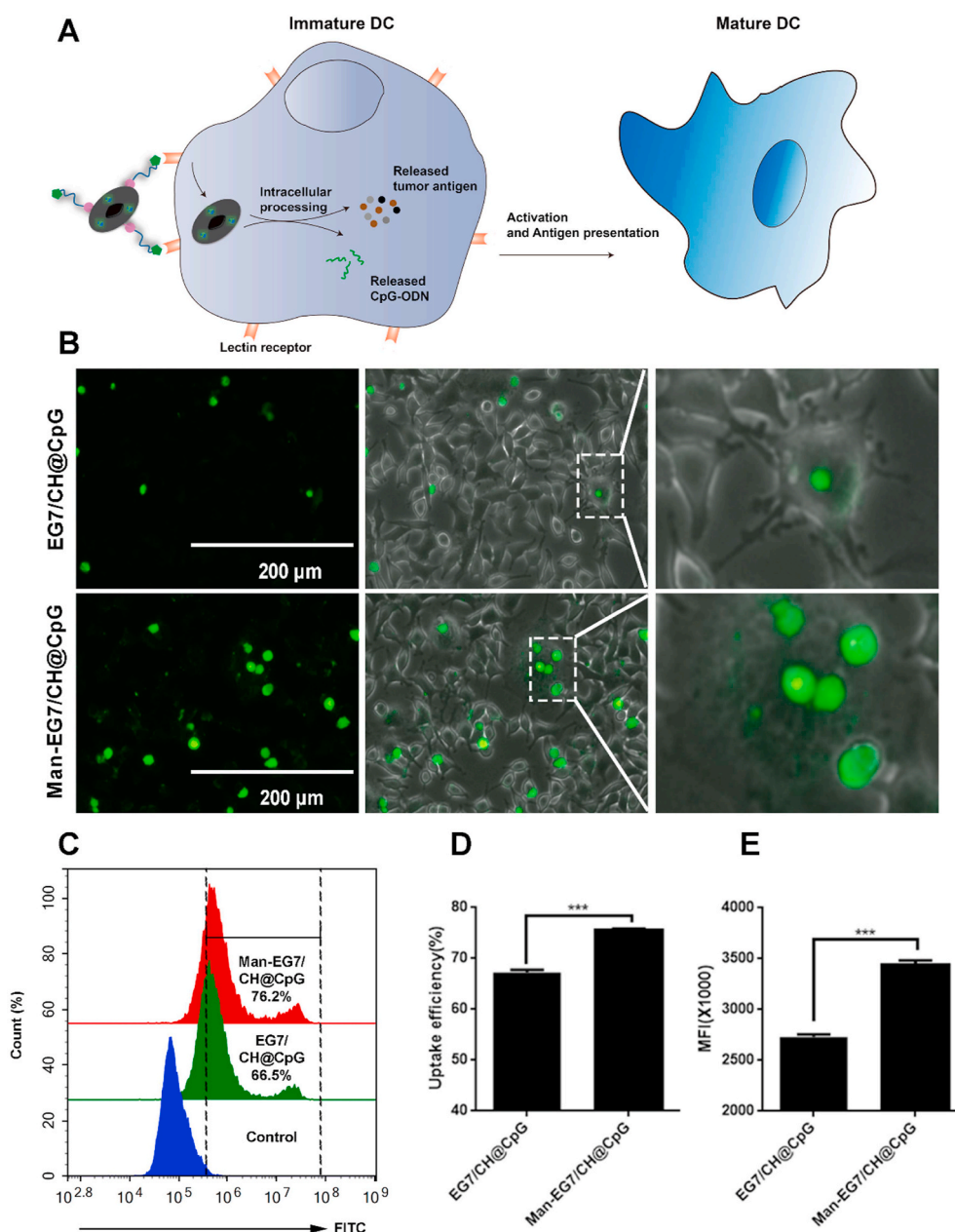
Fig. 2. Uptake characterization of vaccine via BMDCs. (A) Schematic view of the uptake of vaccine via DCs. (B) Fluorescence assay of uptake efficiency by BMDCs of double-improved vaccine (scale bar, 100 μm). (C) Flow cytometry detection of uptake efficiency of Man-EG7/CH@CpG by BMDCs. (D, E) Statistics of BMDCs' uptake efficiency of mono- or double-improved vaccine via flow cytometry detection. The results are shown as mean ± SEM, ***P < 0.001 compared to the related control group by two-tailed Student's *t*-test.

on the surface of APCs (DCs), and the results in our assay implied that interstitial DCs might capture the mannose-binding Man-EG7/CH@CpG vaccine DCs and indirectly enter the lymph node or are directly taken by resident DCs in the lymph nodes, which results in an enhanced immune response [50].

3.5. Man-EG7/CH@CpG vaccine promotes endogenous lymphocyte proliferation in vitro and effectively prevents EG7 tumor formation

To detect the immune activation of Man-EG7/CH@CpG, the proliferation of the lymphocytes from the vaccinated mice was tested in vitro via CFSE labeling method. The population of $CD3^+CFSE^+$ T cells, which represents the activated T lymphocytes, was analyzed. The rate of proliferation of T cells was significantly enhanced by Man-EG7/CH@CpG immunization compared to the control. Importantly,

compared with EG7 or CH@CpG vaccination group, T cells of the Man-EG7/CH@CpG group proliferated twofold more after stimulation by antigen in vitro (Fig. 5E). To further examine the antitumor function of the Man-EG7/CH@CpG vaccine, we used a lymphoma prevention model (Fig. 5A). Mice were immunized with PBS, CH@CpG, EG7, EG7/CH@CpG, or Man-EG7/CH@Cp three times, and then 1×10^6 EG7 cells were inoculated on the back of mice after 7 days. To calculate the tumor formation rate of different treatment groups, mice were observed daily. Six days after inoculation, tumors were formed in all animals of the PBS group, and the percentages of mice with tumors were 75%, 25%, and 0% in the CH@CpG, EG7/CH@CpG, and Man-EG7/CH@CpG groups, respectively. Following with the progress of tumor growth, all mice of the CH@CpG group formed tumors sixteen days after inoculation and 75% of the mice in the EG7 group established tumors eighteen days after inoculation, and for the EG7/CH@CpG group, tumor
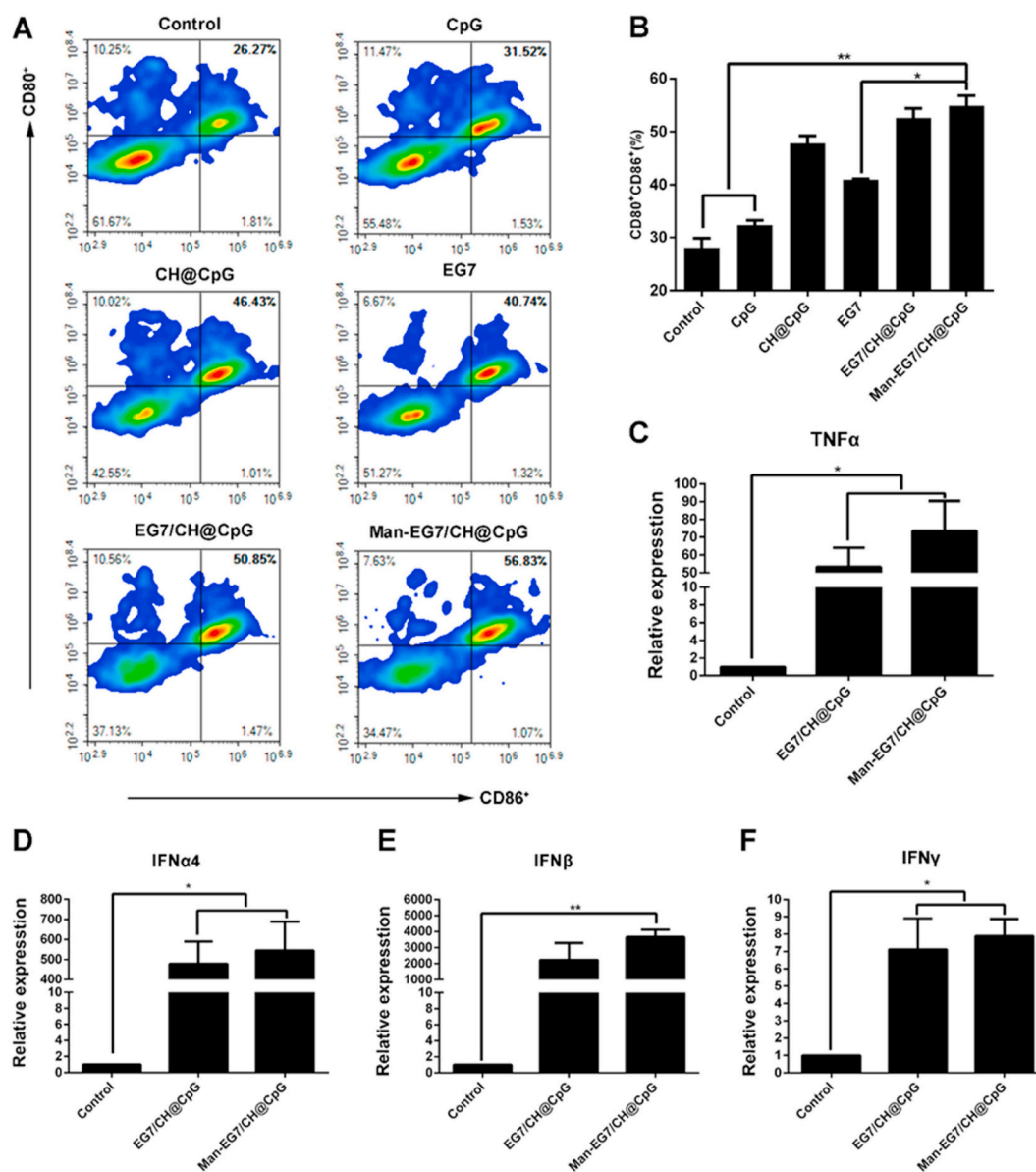
Fig. 3. Man-EG7/CH@CpG vaccine efficiently activates BMDCs in vitro. (A) Mature situations of BMDCs in different stimulation conditions. (B) Statistics of mature efficiency after the different stimulations. (C) The mRNA expression of cytokine of tumor necrosis factor (TNFα) was detected by a qPCR assay. (D–F) The mRNA expression of interferons (IFNα4, IFNβ, and IFNγ) was detected by qPCR. The results are shown as mean ± SEM, *$P < 0.5$, **$P < 0.01$.

formation stayed at 25% rate. It is encouraging that we did not find tumors in the Man-EG7/CH@CpG treatment group during the observation period (Supplementary Fig. 5), which indicates a potential antitumor effect for the therapy in the murine model. Eighteen days after inoculation, mice were sacrificed for further management, and the results of tumor formation and growth were consistent with the tumor formation rate assay (Fig. 5B and C). As significant immune cells (DC or T cell) are located in lymph node, studies have revealed that immune cells in lymph node may be proliferated and activated following with the effective uptake of vaccine, and intense immune response in which may enlarge the lymph nodes of mice [63–65]. We preliminarily detected the immune response in mice, especially in the lymph nodes (lymph nodes of mice in each group were detached, and the representative lymph nodes were captured and are presented in Fig. 5D). Compared with the EG7/CH@CpG group, the size of the lymph nodes in the Man-EG7/CH@CpG group has nearly doubled, frozen sections of lymph nodes stained with DAPI also confirmed this result.

3.6. Man-EG7/CH@CpG vaccine can inhibit and delay tumor growth in the lymphoma treatment model

Next, we examined the antitumor effect of Man-EG7/CH@CpG and the protocol is shown in Fig. 6A. Twenty-two days after inoculation, mice were sacrificed, and tumors were separated for further analysis. Tumors in the CH@CpG and EG7 treatment groups were almost the same as in the PBS group. Tumors of the EG7/CH@CpG treatment group decreased a little, and in the Man-EG7/CH@CpG treatment group, tumors effectively diminished (Fig. 6C). Except for the Man-EG7/CH@CpG vaccine treatment, no significant difference in tumor growth volumes was observed between the control group and other treatment groups (Fig. 6B). The results of tumor weight showed that the tumor inhibition rate in Man-EG7/CH@CpG treatment could reach 66%, which was consistent with tumor growth curves (Fig. 6D). Our results indicate that vaccines based on whole tumor cells can be enhanced by decoration with multiple molecules to improve the immunocompetence and effectively boost the antitumor function in vivo.
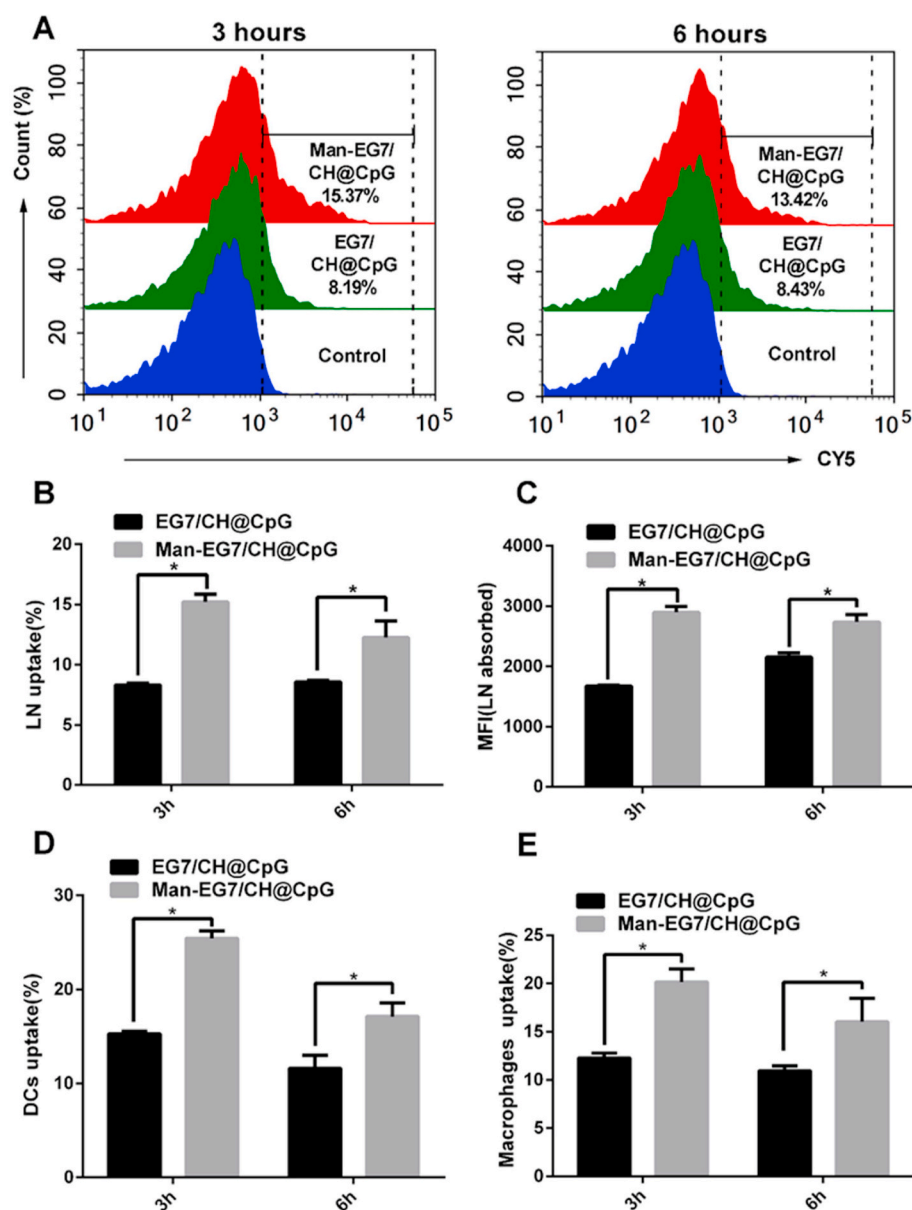
Fig. 4. Double-improved Man-EG7/CH@CpG vaccine enhances APCs targeting efficiency in the lymph nodes. (A) Enhanced targeting effect of lymph node of tumor cell-based vaccine, which was decorated with DCs' targeting ligand. (B, C) Statistics of lymph node uptake efficiency and MFI, which was evaluated by flow cytometry at a separate time point. (D) The uptake situation of the vaccine at each time point by resident DCs was tested. (E) The uptake situation of the vaccine at each time point by resident macrophages was examined. *$P < 0.5$ compared to the related control group by two-tailed Student's *t*-test. For all experiments, the results are shown as mean ± SEM.

3.7. Combined with a chemotherapeutic drug, man-EG7/CH@CpG vaccine inhibits lymphoma growth of mice with high-efficiency

To optimize the therapeutic efficacy further, we combined chemotherapy with the Man-EG7/CH@CpG vaccine to remarkably inhibit tumor growth. The detailed dosage regimens are shown in the experimental section (Fig. 7A). No significant difference in tumor growth was found between PBS and DOX treatment alone; tumor growth was slightly and equally inhibited in CH@CpG and EG7 combined with DOX groups (Fig. 7B). In addition, for the group of EG7/CH@CpG or Man-EG7/CH@CpG combined with DOX, tumor growth was significantly inhibited. Compared with the EG7/CH@CpG-DOX combination administration, some tumors of mice in the Man-EG7/CH@CpG-DOX combination group had indeed completely regressed, and the tumor inhibition rate in the Man-EG7/CH@CpG-DOX treatment can reach 85% (Fig. 7C and D).The tumor growth curves of mice in each group shown in Fig. 7E are consistent with the tumor weight result (Red dashed line means the average tumor volume). For the survival study in a relatively long period, Man-EG7/CH@CpG and DOX combination group effectively prolonged the survival of mice (nearly ten days more than the control group, Fig. 7F). Our combination therapeutic method

obtained a favorable antitumor effect in the lymphoma mice model, which may offer a new therapeutic venue to treat tumors.

3.8. The combination of DOX and man-EG7/CH@CpG vaccine can trigger the adaptive immune response and reverse the immunosuppression state

As primary cytotoxicity cells, TILs are considered a manifestation of an antitumor reaction [66,67]. The combinations of Man-EG7/CH@CpG and DOX showed evident antitumor efficiency in the EG7 lymphoma model. Thus, we investigated the mechanism of the antitumor effect further. Immunofluorescence was used to measure the levels of CD3 and CD8 in EG7 tumor tissue. According to our assay, mice in the Man-EG7/CH@CpG and DOX combination group showed more CD3$^+$CD8$^+$ cells than other groups, which indicates the activation of TILs in the tumor area (Fig. 8A). Adaptive immunity plays a vital role in tumor immunotherapy, and for most unsuccessful immunotherapies, the immune microenvironment of the body is on the suppression state [68,69]. For the assay of the immune microenvironment, lymphocytes were separated from the murine spleens or lymph nodes and co-stained with CD3, CD4, and FOXP3 (markers of Tregs), or CD3, CD8, and IFNγ (markers of CTLs). As shown in Fig. 8B, the
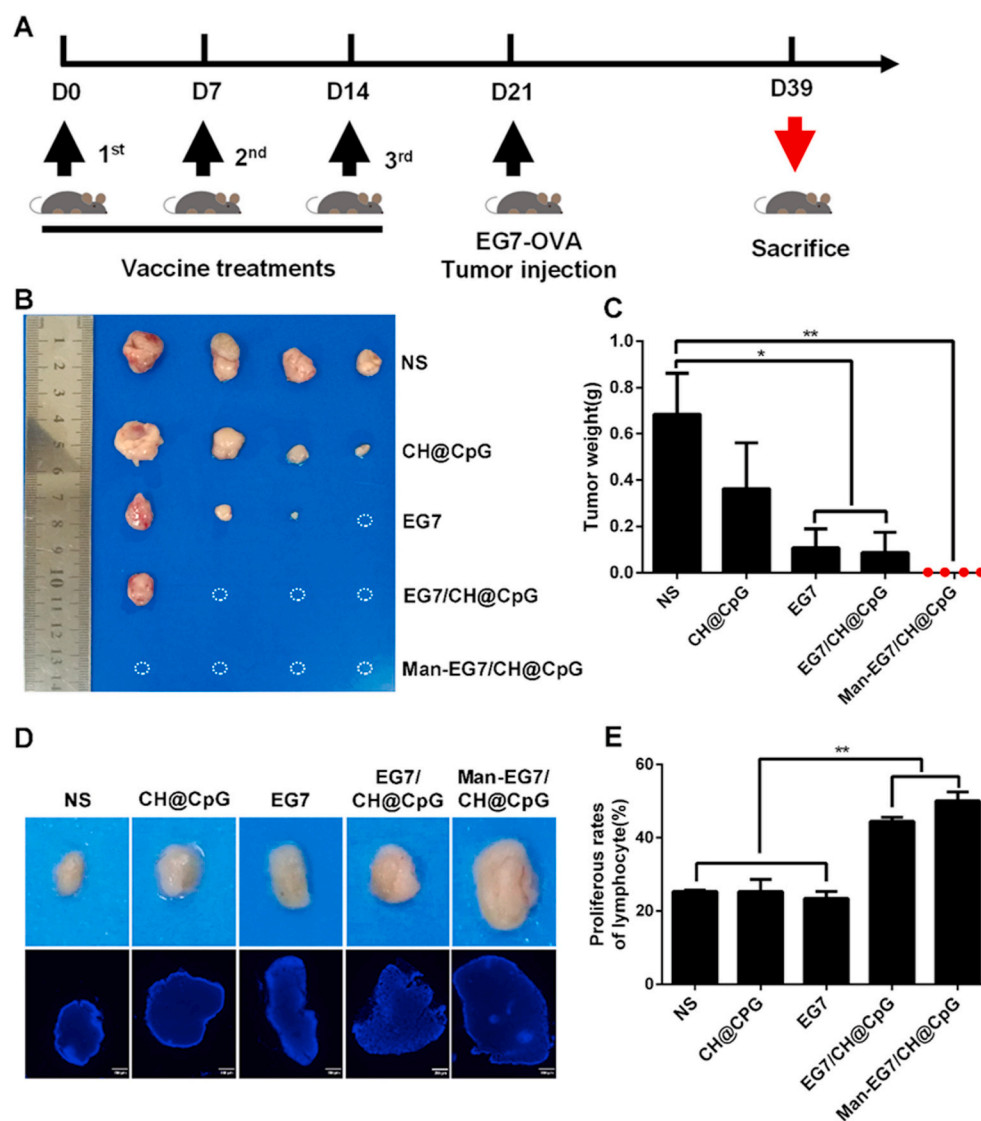
Fig. 5. The Man-EG7/CH@CpG vaccine promotes endogenous T lymphocyte proliferation and effectively inhibits tumor formation in the lymphoma prevention model. (A) Schematic diagram of the vaccination protocol. (B) Representative images of tumor formation of the EG7 prevention model (n = 4 for each group). The dotted circles show the blank of tumor growth. (C) Tumor weight in different treatments for the prevention of EG7 lymphoma. (D) Representative images of lymph node of mice (n = 4 for each group, scale bars, 100 μm). (E) The proliferation of splenic lymphocytes of each group in vitro. *P < 0.5, **P < 0.01, compared to the related control group by two-tailed Student's *t*-test. Error bars represent SEM for n = 4.

population of the $CD3^+CD4^+FOXP3^+$ in Man-EG7/CH@CpG and DOX combination group decreased nearly two-fold compared to the other groups, which means that the combination therapy weakened the immunosuppression. Furthermore, the proportion of $CD3^+CD8^+IFN\gamma^+$ T cells in the combination group increased almost two-fold compared to the other groups. Lymphocytes separated from the murine lymph nodes were also tested, and the observations were consistent with the role of splenic lymphocytes (Fig. 8C). Our results suggest that the combination of chemotherapy and immune activation contributes to the antitumor effect and support the use of this combined therapy.

3.9. The safety evaluation of the immune-chemo combination therapy

We also preliminarily evaluated the safety of this combined antitumor method. In macroscopic changes, no relevant adverse effects, such as skin ulcerations, ruffled fur, or toxic death, were found (data not shown). We further detected pathologic lesions in the heart, lungs, spleen, liver, and kidneys of each group, and no microscopic toxic signs were found (Fig. 9A), which means that no evidence for autoimmunity was gathered. The body weight curves of the Man-EG7-CH@CpG and DOX inoculated group were similar to those of the other groups (Fig. 9B). Since toxicity correlates with weight loss, these data indicate a lack of toxicity in the groups treated with the DOX drug and/or the Man-EG7/CH@CpG vaccine. We also did not find a risk of tumor

formation due to the Man-EG7/CH@CpG vaccine (Supplementary Fig. 6). Our results indicate that this combination therapy is an effective and safe lymphoma treatment method. This therapy should be further studied and could potentially be applied in preclinical or clinical lymphoma research.

4. Discussion

A whole tumor cell vaccine provides a vast repertoire of antigens released from the dying tumor cells, which could theoretically initiate concurrent CD4 and CD8 T cells based antitumor immunity along with antibodies related to the tumor reaction. This strategy has been studied and applied for a long time [26,70]. Recently, a meta-analysis of nearly 200 clinical trials reported that tumor cell vaccines have higher response rates (~8%) than subunit and peptide vaccines (~4%) [71]. However, the level of purity and content of tumor-specific antigen is below the optimal levels to trigger a favorable antitumor effect, which indicates that new strategies to develop tumor cell vaccines are required [31]. Feasible improvements such as genetically modifying strategies and biomolecules or adjuvants engineering operations led to the generation of vaccines that produce GM-CSF or TGF-β classified cytokines spontaneously or boosted the amount of antigenic component of the vaccine [32,33,72].

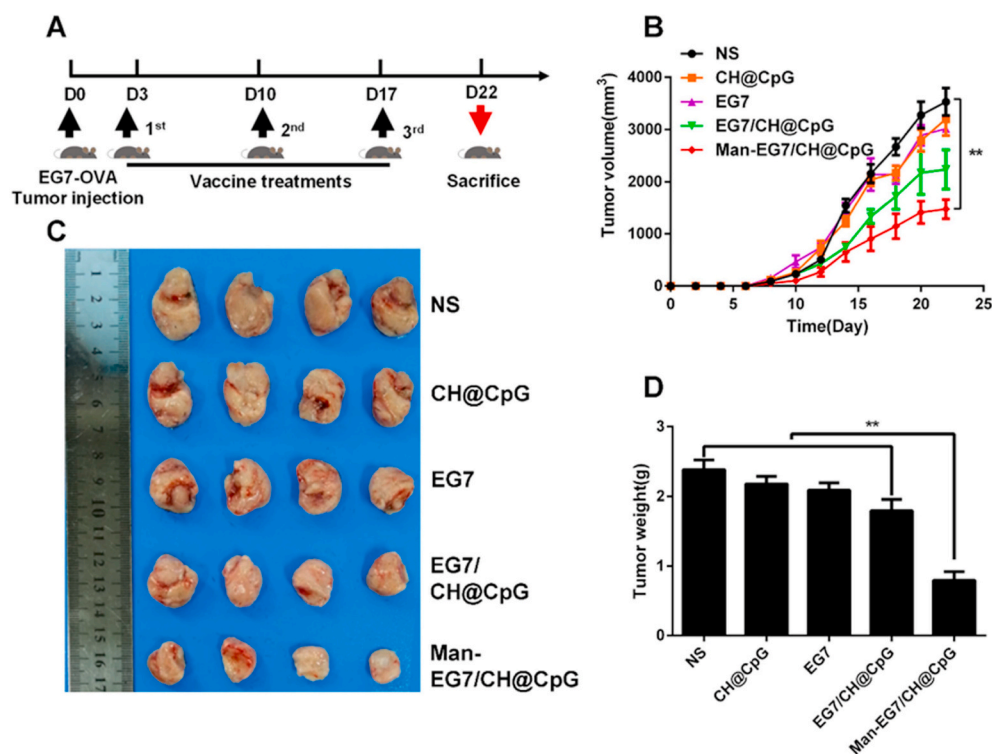Toll-like receptor (TLR) agonists were widely used as adjuvants in

Fig. 6. The Man-EG7/CH@CpG vaccine induces a significant antitumor effect in the lymphoma treatment model. (A) Schematic diagram of the treatment of lymphoma in mice. (B) Tumor volume of whole groups versus time, and tumor volume was monitored every two days. (C) Tumor images of each treatment group (n = 4 for each group). (D) Tumor weight in different treatments in the transplantable EG7 lymphoma model (Student's t-test, **P < 0.01).

recent years [42,73], among which, TLR9 agonists was developed especially. Toll-like receptor 9 (TLR9) is expressed mainly on immune cells, for example, macrophages and dendritic cells. Growing evidence suggests that the activation of TLR9 plays a vital role in initiating the innate immune response and inducing an adaptive immune response [74]. The potent immune response elicited from the pathogens-derived CpG oligonucleotide (CpG-ODN) has unambiguously revealed it as a TLR9 ligand [47]. A cell-particle hybrid contains tumor cells, and the TLR9 ligand was tested in low-volume melanoma and prostate cancer disease [75]. A similar whole tumor cell vaccine for melanoma and colon carcinoma comprised immunogenic tumor cells and TLR9 ligands [76]. Our study, however, internalized the CpG-ODN into tumor cells, and comprehensively specified the immunocompetence in vitro and the antitumor efficacy in vivo. Notably, the Man-EG7/CH@CpG vaccine that we engineered combines the tumor cell with TLR9 ligand and is further decorated with a mannose ligand, which excited the TLR9 pathway and targeted dendritic cells for amplifying the tumor-specific cytotoxic lymphocyte (CTL) effect. The critical design of our vaccine revolves around the access of CpG-ODN and linkage of mannose ligand to whole tumor cells. Our report illustrates that the chitosan-coated CpG-ODN (CH@CpG) was easily absorbed into cells. Via affinity interaction, DSPE-PEG-Mannose establishes tight links to lethally irradiated tumor cells. The man-EG7/CH@CpG vaccine was eventually manufactured.

Although the immunocompetence of the whole tumor cell vaccine was enhanced, and there was an antitumor effect, it may be too modest against rapidly advancing and developing tumor cells. Our treatment results may be restrictive when the vaccine is administered after three days interval from inoculation, i.e., tumor cells may have adapted to a new environment, and immune tolerance could be already established at this point [77–79]. Future studies will directly test how to administrate the vaccine to enhance the cross-priming effect, which is decisive in active immunotherapy, for example, timely administration of vaccine (administered after one day interval from inoculation) can be adopted [80,81]. The limitations of our report also include the lack of a mechanism for the increased immunocompetence of adjuvant compound Man-EG7/CH@CpG vaccine. We speculate that our novel vaccine may

serve as a CpG-ODN depot, and by the engagement of the DCs targeting function, the TLR9 signal pathway is activated, then it may promote the secretion of cytokines (e.g. TNF-α, IFN-γ) to prime CTLs or inhibiting the secretion of chemokines and cytokines (e.g. CCL5, IL-6). to interfere Tregs' development [74,82–85]. These possible mechanisms need to be further assayed in tumor treatment models of TLR9 gene knockout mouse in future studies.

Numerous treatment options have been used for NHL, including CHOP and EPOCH chemotherapy regimens, which are first-line treatments. However, a weak curative effect was achieved [86]. Moreover, in the process of rapid tumor progression, the antitumor immune response mediated by immunotherapy only is insufficient to prevent the highly proliferative tumor cells, which generates unsatisfactory treatment results [87]. Concerning this aspect, chemotherapeutic agents can develop a positive function, which acts as a preferred option in tumor disease therapies [88]. Thus, the combination of the immunotherapeutic regimen with the chemotherapy administration has been tried, and a synergistic treatment effect was already demonstrated [89,90]. As for NHL, the strategy of anti-CD20 monoclonal antibody-based immunotherapy combined with chemotherapy improved lymphoma therapy, but the promoting effect was limited [91]. Man-EG7/CH@CpG, which was shown to have enhanced immunocompetence and can activate a delicate antitumor response, is well suited for combination with chemotherapeutic drugs (DOX, one of the first line adopted drugs in lymphoma treatment) to improve the lymphoma treatment further. Recent studies have found that DOX can induce the ICD of tumor cells to stimulate the antitumor immune function, which was illustrated by clinical data from patients [88]. The results of the combined therapy in lymphoma model are encouraging. Our future explorations will focus on the state of recurrence after combined treatment and the potential significance of the combination scheme using the improved vaccine to cure multiple tumors.

5. Conclusion

In our study, we report a novel tumor cell vaccine, Man-EG7/CH@CpG, which composed with tumor antigen, TLR9 ligand and DCs'
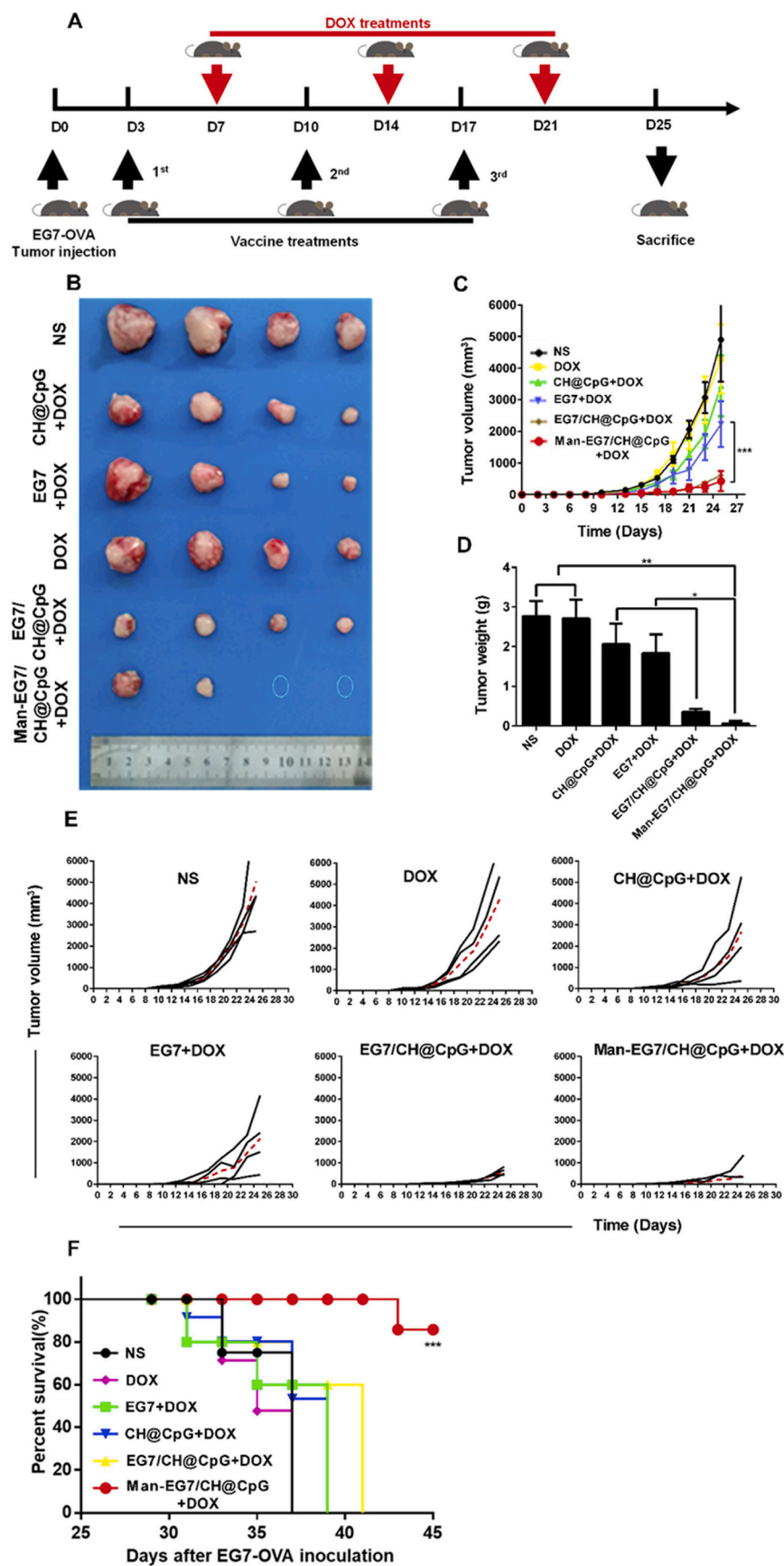
Fig. 7. The combination of chemotherapeutic drug and Man-EG7/CH@CpG vaccine induced a synergetic anti-tumor effect in vivo. (A) Schematic diagram of the establishment of the lymphoma model and the administration of immune-chemotherapy. (B) Tumor images of each group harvested from animals after immuno-chemotherapy (n = 4 for each group, a white dashed circle means the absence of tumors). (C) Tumor volume of whole groups versus time monitored every two days. (D) Tumor weights of each group. (E) Tumor volume of individual groups versus time was monitored every two days. (F) Survival curve of different treatments in established tumors. The group of Man-EG7/CH@CpG vaccine and DOX drug exhibited an overall survival benefit. (n = 4, *P < 0.05, **P < 0.01, ***P < 0.001.).
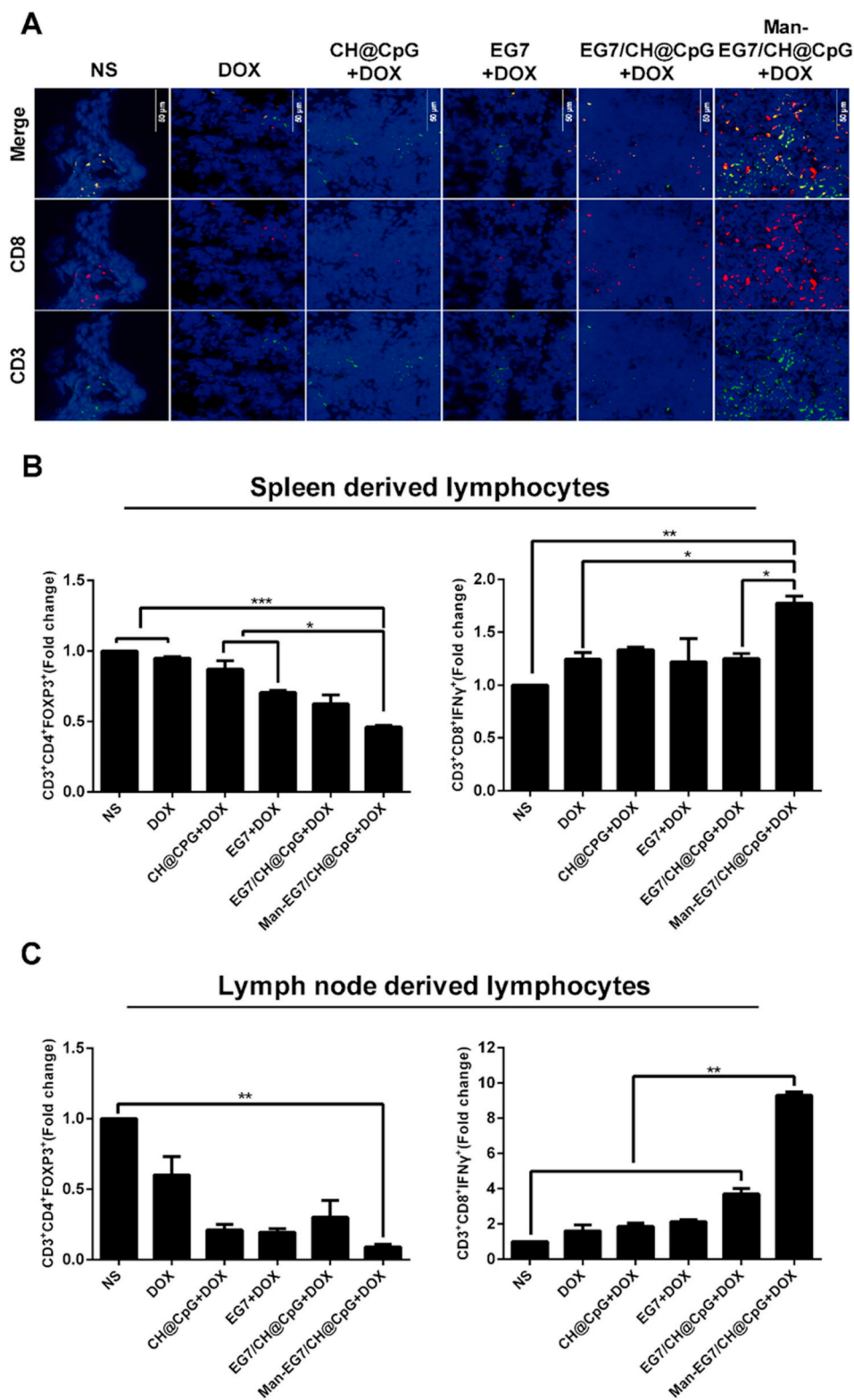
Fig. 8. Activation of antitumor immune response by Man-EG7/CH@CpG vaccine combination with a chemotherapeutic drug. (A) The fluorescent images of tumor infiltration lymphocytes (CD3$^+$CD8$^+$) in tumor tissues from different therapeutic EG7 lymphoma mice. (B) The number of spleen-derived suppressive immune cells (CD3$^+$/CD4$^+$/FOXP3$^+$ T cells) and activated immune cells (CD3$^+$/CD8$^+$/IFNγ$^+$ T cells) in the lymphoma treatment model. (C) The number of lymph node-derived suppressive immune cells (CD3$^+$/CD4$^+$/FOXP3$^+$ T cells) and activated immune cells (CD3$^+$/CD4$^+$/IFNγ$^+$ T cells) in the lymphoma treatment model. All experimental data were analyzed as mean ± SEM and *P < 0.05, **P < 0.01, ***P < 0.001 (Student's *t*-test).

targeting ligand, triggers an adaptive immune response and has excellent tumor rejection ability after subcutaneous immunization in a preventive xenograft lymphoma mouse model. Moreover, to improve the curative effect of immunotherapy alone, we added the DOX drug by tail vein injection during the process of vaccine administration. The scheme evidently increased tumor inhibition rate and prolonged the survival period of the mice. In addition, no major risks or adverse reactions were detected, which suggests that this treatment scheme is safe. In summary, our findings revealed the immunocompetence of a new vaccine, namely its antitumor effect for immunotherapy, and highlighted the benefits of combining immunotherapy with chemotherapy.
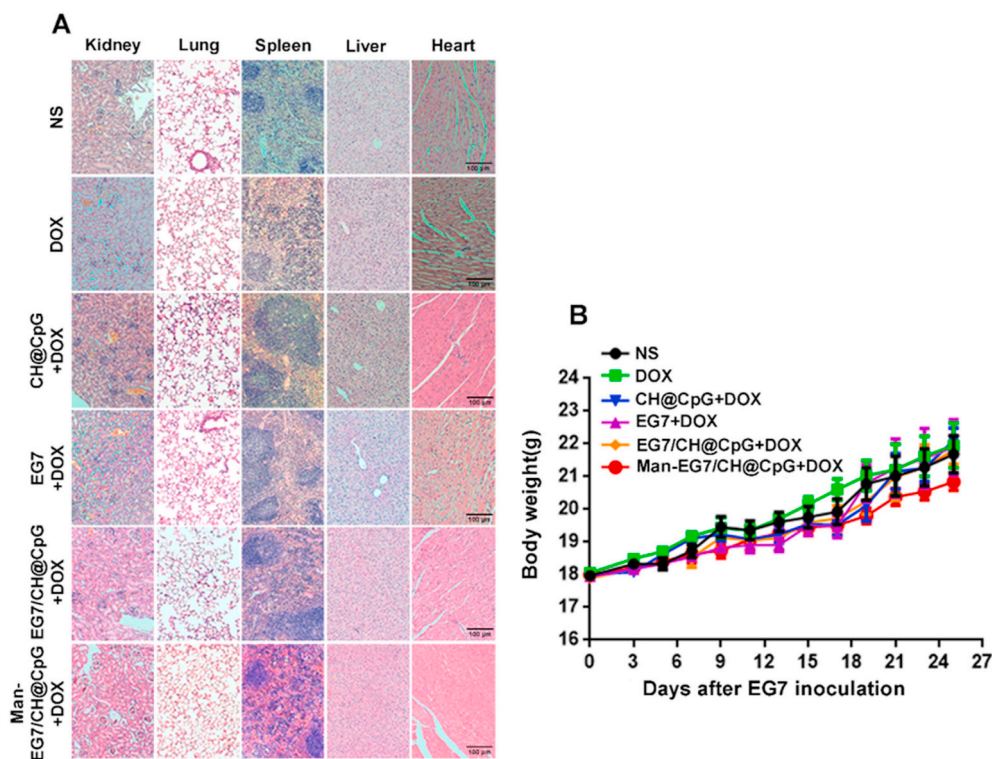
Fig. 9. Safety evaluation of Man-EG7/CH@CpG vaccine combination with a chemotherapeutic drug. (A) Representative HE staining images of organs harvested from animals in each treatment group (scale bar, 100 μm). (B) Weight changing curves of mice after different treatments (n = 4 for each group).

Credit Author Statement

Declaration of competing interest

The authors declare that they have no known competing financial interests or personal relationships that could have appeared to influence the work reported in this paper.

Acknowledgements

Appendix A. Supplementary data

Supplementary data to this article can be found online at https://doi.org/10.1016/j.bioactmat.2020.09.002.

Abbreviations list

NHL	Non-Hodgkin lymphoma
Man	DSPE-PEG-Mannose
CH@CpG	chitosan-coated CpG complex
ACT	adoptive cellular therapy
ICBs	Immune-Checkpoint Blocker
ICD	immunogenic cell death
DOX	doxorubicin
CRS	cytokine release syndrome
Lipo3K	Lipofectamine ™ 3000
TLR	toll-like receptor
DOTAP	1,2-dioleoyl-3-trimethylammonium-propane
CFSE	carboxyfluorescein succinimidyl amino ester
MFI	mean fluorescence intensity
CTLs	cytotoxic lymphocyte
Tregs	regulatory T cells
TILs	tumor-infiltrating lymphocytes

References

[1] J.O. Armitage, R.D. Gascoyne, M.A. Lunning, F. Cavalli, Non-Hodgkin Lymphoma, (2017).

[2] K.R. Shankland, J.O. Armitage, B.W. Hancock, Non-Hodgkin Lymphoma, (2012).

[3] R.L. Siegel, K.D. Miller, A. Jemal, Cancer statistics, 2020, CA, A Cancer Journal for Clinicians 70 (2020) 7–30.

[4] C. Fitzmaurice, D. Abate, N. Abbasi, H. Abbastabar, F. Abd-Allah, O. Abdel-Rahman, A. Abdelalim, A. Abdoli, I. Abdollahpour, A. Abdulle, N. Dereje, H. Niguse, L. Abu-Raddad, A. Abualhasan, A. Isaac, S. Advani, M. Afarideh, M. Afshari, M. Aghaali, A. Ghajar, Global, regional, and national cancer incidence, mortality, years of life lost, years lived with disability, and disability-adjusted life-years for 29 cancer groups, 1990 to 2017 A systematic analysis for the global burden of disease

study, JAMA Oncology 5 (2019) 1749–1768.

[5] T.J. Stillwell, R.C. Benson Jr., Cyclophosphamide-induced hemorrhagic cystitis. A review of 100 patients, Cancer 61 (1988) 451–457.

[6] S. Zhang, X. Liu, T. Bawa-Khalfe, L.-S. Lu, Y.L. Lyu, L.F. Liu, E.T.H. Yeh, Identification of the molecular basis of doxorubicin-induced cardiotoxicity, Nat. Med. 18 (2012) 1639–1642.

[7] A. Areti, V.G. Yerra, V. Naidu, A. Kumar, Oxidative stress and nerve damage: role in chemotherapy induced peripheral neuropathy, Redox Biol 2 (2014) 289–295.

[8] S.J. Taylor, J.M. Duyvestyn, S.A. Dagger, E.J. Dishington, C.A. Rinaldi, O.M. Dovey, G.S. Vassiliou, C.S. Grove, W.Y. Langdon, Preventing chemotherapy-induced myelosuppression by repurposing the FLT3 inhibitor quizartinib, Sci. Transl. Med. 9 (2017).

[9] V. Poeschel, G. Held, M. Ziepert, M. Witzens-Harig, H. Holte, L. Thurner, P. Borchmann, A. Viardot, M. Soekler, U. Keller, C. Schmidt, L. Truemper, R. Mahlberg, R. Marks, H.-G. Hoeffkes, B. Metzner, J. Dierlamm, N. Frickhofen, M. Haenel, A. Neubauer, M. Kneba, F. Merli, A. Tucci, P. de Nully Brown, M. Federico, E. Lengfelder, A. di Rocco, R. Trappe, A. Rosenwald, C. Berdel, M. Maisenhoelder, O. Shpilberg, J. Amam, K. Christofyllakis, F. Hartmann, N. Murawski, S. Stilgenbauer, M. Nickelsen, G. Wulf, B. Glass, N. Schmitz, B. Altmann, M. Loeffler, M. Pfreundschuh, Four versus six cycles of CHOP chemotherapy in combination with six applications of rituximab in patients with aggressive B-cell lymphoma with favourable prognosis (FLYER): a randomised, phase 3, non-inferiority trial, Lancet 394 (2019) 2271–2281.

[10] M.F. Sanmamed, L. Chen, A paradigm shift in cancer immunotherapy: from enhancement to normalization, Cell 175 (2018) 313–326.

[11] C. Zhang, K. Pu, Molecular and nanoengineering approaches towards activatable cancer immunotherapy, Chem. Soc. Rev. 49 (2020).

[12] Pu K., Li J., Luo Y., Electromagnetic nanomedicines for combinational cancer immunotherapy, Angew. Chem. Int. Ed., doi:10.1002/anie.202008386.

[13] J. Li, D. Cui, J. Huang, S. He, Z. Yang, Y. Zhang, Y. Luo, K. Pu, Organic semiconducting pro-nanostimulants for near-infrared photoactivatable cancer immunotherapy, Angew. Chem. 58 (2019) 12680–12687.

[14] W.C.-W. Suen, W.Y.-W. Lee, K.-T. Leung, X.-H. Pan, G. Li, Natural killer cell-based cancer immunotherapy: a review on 10 Years completed clinical trials, Canc. Invest. 36 (2018) 431–457.

[15] A. Holzinger, M. Barden, H. Abken, The growing world of CAR T cell trials: a systematic review, Cancer Immunology, Immunotherapy 65 (2016) 1433–1450.

[16] N. Abdel Karim, K. Kelly, Role of targeted therapy and immune checkpoint blockers in advanced non-small cell lung cancer: a review, Oncol. 24 (2019) 1270–1284.

[17] S.M. Ansell, A.M. Lesokhin, I. Borrello, A. Halwani, E.C. Scott, M. Gutierrez, S.J. Schuster, M.M. Millenson, D. Cattry, G.J. Freeman, S.J. Rodig, B. Chapuy, A.H. Ligon, L. Zhu, J.F. Grosso, S.Y. Kim, J.M. Timmerman, M.A. Shipp, P. Armand, PD-1 blockade with nivolumab in relapsed or refractory Hodgkin's lymphoma, N. Engl. J. Med. 372 (2015) 311–319.

[18] K. Perica, J.C. Varela, M. Oelke, J.P. Schneck, Adoptive T cell immunotherapy for cancer, Rambam Maimonides Medical Journal 6 (2015).

[19] S.S. Kenderian, M. Ruella, O. Shestova, M.Y. Kim, M. Klichinsky, F. Chen, N. Kengle, S.F. Lacey, J.J. Melenhorst, C.H. June, Ruxolitinib prevents cytokine release syndrome after CART cell therapy without impairing the anti-tumor effect in a xenograft model, Blood 128 (2016) 652-652.

[20] U. Sahin, E. Derhovanessian, M. Miller, B. Kloke, P. Simon, M. Lower, V. Bukur, A.D. Tadmor, U. Luxemburger, B. Schrors, Personalized RNA mutanome vaccines mobilize poly-specific therapeutic immunity against cancer, Nature 547 (2017) 222–226.

[21] U. Sahin, O. Tureci, Personalized vaccines for cancer immunotherapy, Science 359 (2018) 1355–1360.

[22] A. Terbuch, J. Lopez, Next generation cancer vaccines—make it personal!, Vaccine 6 (2018) 52.

[23] C.A. Klebanoff, N. Acquavella, Z. Yu, N.P. Restifo, Therapeutic cancer vaccines: are we there yet? Immunol. Rev. 239 (2011) 27–44.

[24] S.A. Forbes, D. Beare, P. Gunasekaran, K. Leung, N. Bindal, H. Boutselakis, M. Ding, S. Bamford, C.G. Cole, S. Ward, COSMIC: exploring the world's knowledge of somatic mutations in human cancer, Nucleic Acids Res. 43 (2015) 805–811.

[25] C. Tomasetti, B. Vogelstein, Variation in cancer risk among tissues can be explained by the number of stem cell divisions, Science 347 (2015) 78–81.

[26] A. Sheikhi, A. Jafarzadeh, P. Kokhaei, M. Hojjatfarsangi, Whole tumor cell vaccine adjuvants: comparing IL-12 to IL-2 and IL-15, Iranian Journal of Immunology 13 (2016) 148–166.

[27] E. Zsiros, D. Dangaj, C.H. June, L.E. Kandalaft, G. Coukos, Ovarian cancer chemokines may not be a significant barrier during whole tumor antigen dendritic-cell vaccine and adoptive T-cell immunotherapy, OncoImmunology 5 (2016).

[28] S. Liu, W. Wei, H. Yue, D. Ni, Z. Yue, S. Wang, Q. Fu, Y. Wang, G. Ma, Z. Su, Nanoparticles-based multi-adjuvant whole cell tumor vaccine for cancer immunotherapy, Biomaterials 34 (2013) 8291–8300.

[29] S. Srivatsan, J.M. Patel, E.N. Bozeman, I.E. Imasuen, S. He, D. Daniels, P. Selvaraj, Allogeneic tumor cell vaccines: the promise and limitations in clinical trials, Hum. Vaccines Immunother. 10 (2014) 52–63.

[30] K. Lauber, N. Brix, A. Ernst, R. Hennel, J. Krombach, H. Anders, C. Belka, Targeting the heat shock response in combination with radiotherapy: sensitizing cancer cells to irradiation-induced cell death and heating up their immunogenicity, Canc. Lett. 368 (2015) 209–229.

[31] C.L. Chiang, G. Coukos, L.E. Kandalaft, Whole tumor antigen vaccines: where are we? Vaccine 3 (2015) 344–372.

[32] M. Terra, M. Oberkampf, C. Fayolle, P. Rosenbaum, C. Guillerey, G. Dadaglio, C. Leclerc, Tumor-derived TGFβ alters the ability of plasmacytoid dendritic cells to respond to innate immune signaling, Canc. Res. 78 (2018) 3014–3026.

[33] N. Senzer, M. Barve, J.A. Kuhn, A. Melnyk, P. Beitsch, M. Lazar, S. Lifshitz, M. Magee, J. Oh, S.W. Mill, Phase I trial of "bi-shRNAifurin/GMCSF DNA/autologous tumor cell" vaccine (FANG) in advanced cancer, Mol. Ther. 20 (2012) 679–686.

[34] Q. Liu, H. Wang, G. Li, M. Liu, J. Ding, X. Huang, W. Gao, W. Huayue, A photo-cleavable low molecular weight hydrogel for light-triggered drug delivery, Chin. Chem. Lett. 30 (2019) 485–488.

[35] L. Ma, S. Lv, J. Tang, J. Liu, W. Li, J. Deng, Y. Deng, J. Du, X. Liu, X. Zeng, Study on bioactive molecules involved in extracellular biosynthesis of silver nanoparticles by Penicillium aculeatum Su1, Materials Express 9 (2019) 475–483.

[36] M. Mohammed, K. Yusoh, J. Shariffuddin, Poly(N-vinyl caprolactam) thermoresponsive polymer in novel drug delivery systems: a review, Materials Express 8 (2018) 21–34.

[37] X. Wang, X. Liang, X. Hao, S. Feng, S. Dai, J. An, J. Li, H. Shi, W. Feng, X. Zhang, Bioinspired drug delivery carrier for enhanced tumor-targeting in melanoma mice model, J. Biomed. Nanotechnol. 15 (2019) 1482–1491.

[38] X. Wang, J. Wang, S. Feng, Z. Zhang, C. Wu, X. Zhang, F. Kang, Nano-porous silica aerogels as promising biomaterials for oral drug delivery of paclitaxel, J. Biomed. Nanotechnol. 15 (2019) 1532–1545.

[39] Z. Zeng, K. Pu, Improving Cancer Immunotherapy by Cell Membrane-Camouflaged Nanoparticles, Advanced Functional Materials, n/a 2004397.

[40] C. Zhang, K. Pu, Recent Progress on Activatable Nanomedicines for Immunometabolic Combinational Cancer Therapy, Small Structures, (n/a).

[41] M. Qi, S. Zou, C. Guo, K. Wang, Y. Yu, F. Zhao, H. Fan, Z. Wu, W. Liu, D. Chen, Enhanced in vitro and in vivo anticancer properties by using a nanocarrier for Co-delivery of antitumor polypeptide and curcumin, J. Biomed. Nanotechnol. 14 (2018) 139–149.

[42] Z. Zhou, H. Lin, C. Li, Z. Wu, Recent progress of fully synthetic carbohydrate-based vaccine using TLR agonist as build-in adjuvant, Chin. Chem. Lett. 29 (2018) 19–26.

[43] H. Wang, D.J. Mooney, Biomaterial-assisted targeted modulation of immune cells in cancer treatment, Nat. Mater. 17 (2018) 761–772.

[44] J.R. Ohlfest, B.M. Andersen, A.J. Litterman, J. Xia, C.A. Pennell, L. Swier, A.M. Salazar, M.R. Olin, Vaccine injection site matters: qualitative and quantitative defects in CD8 T cells primed as a function of proximity to the tumor in a murine glioma model, J. Immunol. 190 (2013) 613–620.

[45] A. Bernkop-Schnürch, S. Dünnhaupt, Chitosan-based drug delivery systems, Eur. J. Pharm. Biopharm. 81 (2012) 463–469.

[46] L. Xing, Y. Fan, T. Zhou, J. Gong, L. Cui, K. Cho, Y. Choi, H. Jiang, C. Cho, Chemical modification of chitosan for efficient vaccine delivery, Molecules 23 (2018) 229.

[47] A.M. Krieg, CpG motifs in bacterial DNA and their immune effects, Annu. Rev. Immunol. 20 (2002) 709–760.

[48] J. Scheiermann, D.M. Klinman, Clinical evaluation of CpG oligonucleotides as adjuvants for vaccines targeting infectious diseases and cancer, Vaccine 32 (2014) 6377–6389.

[49] X. Yang, C. Lai, A. Liu, X. Hou, Z. Tang, F. Mo, S. Yin, X. Lu, Anti-tumor activity of mannose-CpG-oligodeoxynucleotides-conjugated and hepatoma lysate-loaded nanoliposomes for targeting dendritic cells in vivo, J. Biomed. Nanotechnol. 15 (2019) 1018–1032.

[50] A. Avrameas, D. Mcilroy, A. Hosmalin, B. Autran, P. Debre, M. Monsigny, A.C. Roche, P. Midoux, Expression of a mannose/fucose membrane lectin on human dendritic cells, Eur. J. Immunol. 26 (1996) 394–400.

[51] C.M. Remsberg, Y. Zhao, J.K. Takemoto, R.M. Bertram, N.M. Davies, M.L. Forrest, Pharmacokinetic evaluation of a DSPE-peg2000 micellar formulation of ridaforolimus in rat, Pharmaceutics 5 (2012) 81–93.

[52] J. Che, C. Okeke, Z.-B. Hu, J. Xu, DSPE-PEG: A Distinctive Component in Drug Delivery System, Current pharmaceutical design, 2015, p. 21.

[53] A. Capasso, J. Lang, T.M. Pitts, K.R. Jordan, C.H. Lieu, S.L. Davis, J.R. Diamond, S. Kopetz, J. Barbee, J. Peterson, B.M. Freed, B.W. Yacob, S.M. Bagby, W.A. Messersmith, J.E. Slansky, R. Pelanda, S.G. Eckhardt, Characterization of immune responses to anti-PD-1 mono and combination immunotherapy in hematopoietic humanized mice implanted with tumor xenografts, Journal for ImmunoTherapy of Cancer 7 (2019) 37.

[54] K.M. Mahoney, P.D. Rennert, G.J. Freeman, Combination cancer immunotherapy and new immunomodulatory targets, Nat. Rev. Drug Discov. 14 (2015) 561–584.

[55] M.B. Lutz, N.A. Kukutsch, A.L. Ogilvie, S. Rossner, F. Koch, N. Romani, G. Schuler, An advanced culture method for generating large quantities of highly pure dendritic cells from mouse bone marrow, J. Immunol. Methods 223 (1999) 77–92.

[56] J.W. Hodge, A. Ardiani, B. Farsaci, A.R. Kwilas, S.R. Gameiro, The tipping point for combination therapy: cancer vaccines with radiation, chemotherapy, or targeted small molecule inhibitors, Semin. Oncol. 39 (2012) 323–339.

[57] J. Lu, X. Liu, Y. Liao, F.B. Salazar, S. Sun, W. Jiang, C.H. Chang, J. Jiang, X. Wang, A.M. Wu, Nano-enabled pancreas cancer immunotherapy using immunogenic cell death and reversing immunosuppression, Nat. Commun. 8 (2017) 1811-1811.

[58] R. Kuai, L.J. Ochyl, K.S. Bahjat, A. Schwendeman, J.J. Moon, Designer vaccine nanodiscs for personalized cancer immunotherapy, Nat. Mater. 16 (2017) 489–496.

[59] D. Nobuoka, T. Yoshikawa, M. Takahashi, T. Iwama, K. Horie, M. Shimomura, S. Suzuki, N. Sakemura, M. Nakatsugawa, H. Sadamori, T. Yagi, T. Fujiwara, T. Nakatsura, Intratumoral peptide injection enhances tumor cell antigenicity recognized by cytotoxic T lymphocytes: a potential option for improvement in antigen-specific cancer immunotherapy, Cancer immunology, immunotherapy, CII 62 (2013) 639–652.

[60] R.L. Sabado, S. Balan, N. Bhardwaj, Dendritic cell-based immunotherapy, Cell Res. 27 (2017) 74–95.

[61] T. Granot, Y. Yamanashi, D. Meruelo, Sindbis viral vectors transiently deliver tumor-associated antigens to lymph nodes and elicit diversified antitumor CD8+ T-cell immunity, Mol. Ther. 22 (2014) 112–122.

[62] P. Barral, P. Polzella, A. Bruckbauer, N. Van Rooijen, G.S. Besra, V. Cerundolo, F.D. Batista, CD169+ macrophages present lipid antigens to mediate early activation of iNKT cells in lymph nodes, Nat. Immunol. 11 (2010) 303–312.

[63] A. Schudel, D.M. Francis, S.N. Thomas, Material design for lymph node drug delivery, Nature Reviews Materials 4 (2019) 415–428.

[64] Z. Xu, S. Ramishetti, Y.C. Tseng, S. Guo, Y. Wang, L. Huang, Multifunctional nanoparticles co-delivering Trp2 peptide and CpG adjuvant induce potent cytotoxic T-lymphocyte response against melanoma and its lung metastasis, J. Contr. Release 172 (2013) 259–265.

[65] S. Kim, Y. Noh, T.H. Kang, J. Kim, S. Kim, S.H. Um, D. Oh, Y. Park, Y.T. Lim, Synthetic vaccine nanoparticles target to lymph node triggering enhanced innate and adaptive antitumor immunity, Biomaterials 130 (2017) 56–66.

[66] R. Salgado, C. Denkert, S. Demaria, N. Sirtaine, F. Klauschen, G. Pruneri, S. Wienert, G.V. Den Eynden, F.L. Baehner, F. Penaultllorca, The evaluation of tumor-infiltrating lymphocytes (TILs) in breast cancer: recommendations by an International TILs Working Group, Ann. Oncol. 26 (2015) (2014) 259–271.

[67] S. Loi, S. Michiels, R. Salgado, N. Sirtaine, V. Jose, D. Fumagalli, P.L. Kellokumpu-Lehtinen, P. Bono, V. Kataja, C. Desmedt, M.J. Piccart, S. Loibl, C. Denkert, M.J. Smyth, H. Joensuu, C. Sotiriou, Tumor infiltrating lymphocytes are prognostic in triple negative breast cancer and predictive for trastuzumab benefit in early breast cancer: results from the FinHER trial, Ann. Oncol. : official journal of the European Society for Medical Oncology 25 (2014) 1544–1550.

[68] A. Marabelle, H.E. Kohrt, I. Sagivbarfi, B. Ajami, R.C. Axtell, G. Zhou, R. Rajapaksa, M.R. Green, J. Torchia, J. Brody, Depleting tumor-specific Tregs at a single site eradicates disseminated tumors, J. Clin. Invest. 123 (2013) 2447–2463.

[69] A. Serrels, T. Lund, B. Serrels, A. Byron, R.C. Mcpherson, A. Von Kriegsheim, L. Gomezcuadrado, M. Canel, M. Muir, J.E. Ring, Nuclear FAK controls chemokine transcription, Tregs, and evasion of anti-tumor immunity, Cell 163 (2015) 160–173.

[70] J. Li, A.V. King, S.L. Stickel, K.E. Burgin, X. Zhang, T.E. Wagner, Y. Wei, Whole tumor cell vaccine with irradiated S180 cells as adjuvant, Vaccine 27 (2009) 558–564.

[71] M.A. Neller, J.A. López, C.W. Schmidt, Antigens for cancer immunotherapy, Semin. Immunol. 20 (2008) 286–295.

[72] S. Park, J.H. Zheng, V.H. Nguyen, S. Jiang, D. Kim, M. Szardenings, J. Min, Y. Hong, H.E. Choy, J. Min, RGD peptide cell-surface display enhances the targeting and therapeutic efficacy of attenuated salmonella-mediated cancer therapy, Theranostics 6 (2016) 1672–1682.

[73] Z. Lu, L. Xu, N. He, F. Huang, T. Xu, L. Li, Y. Zhang, L. Zhang, Cy5.5-MSA-G250 nanoparticles (CMGNPs) induce M1 polarity of RAW264. 7 macrophage cells via TLR4-dependent manner, Chin. Chem. Lett. 30 (2019) 1320–1324.

[74] F. Steinhagen, T. Kinjo, C. Bode, D.M. Klinman, TLR-based immune adjuvants, Vaccine 29 (2011) 3341–3355.

[75] K.K. Ahmed, S.M. Geary, A.K. Salem, Surface engineering tumor cells with adjuvant-loaded particles for use as cancer vaccines, J. Contr. Release 248 (2017) 1–9.

[76] Y. Fan, R. Kuai, Y. Xu, L.J. Ochyl, D.J. Irvine, J.J. Moon, Immunogenic cell death amplified by Co-localized adjuvant delivery for cancer immunotherapy, Nano Lett. 17 (2017) 7387–7393.

[77] A.K. Palucka, L.M. Coussens, The basis of oncoimmunology, Cell 164 (2016) 1233–1247.

[78] H.E. Barker, J.T. Paget, A.A. Khan, K.J. Harrington, The tumour microenvironment after radiotherapy: mechanisms of resistance and recurrence, Nat. Rev. Canc. 15 (2015) 409–425.

[79] A.C. Anderson, N. Joller, V.K. Kuchroo, Lag-3, tim-3, and TIGIT: Co-inhibitory receptors with specialized functions in immune regulation, Immunity 44 (2016) 989–1004.

[80] M.J. Bevan, Cross-priming for a secondary cytotoxic response to minor h antigens with h-2 congenic cells which do not cross- -react in the cytotoxic assay, J. Exp. Med. 143 (1976) 1283–1288.

[81] M. Azuma, T. Ebihara, H. Oshiumi, M. Matsumoto, T. Seya, Cross-priming for antitumor CTL induced by soluble Ag + polyI:C depends on the TICAM-1 pathway in mouse CD11c+/CD8α+ dendritic cells, OncoImmunology 1 (2012) 581–592.

[82] A. Kimura, T. Kishimoto, IL-6: regulator of treg/Th17 balance, Eur. J. Immunol. 40 (2010) 1830–1835.

[83] A. Serrels, T. Lund, B. Serrels, A. Byron, R.C. McPherson, A. von Kriegsheim, L. Gómez-Cuadrado, M. Canel, M. Muir, J.E. Ring, E. Maniati, A.H. Sims, J.A. Pachter, V.G. Brunton, N. Gilbert, S.M. Anderton, R.J.B. Nibbs, M.C. Frame, Nuclear FAK controls chemokine transcription, Tregs, and evasion of anti-tumor immunity, Cell 163 (2015) 160–173.

[84] J. Lu, X. Liu, Y.-P. Liao, F. Salazar, B. Sun, W. Jiang, C.H. Chang, J. Jiang, X. Wang, A.M. Wu, H. Meng, A.E. Nel, Nano-enabled pancreas cancer immunotherapy using immunogenic cell death and reversing immunosuppression, Nat. Commun. 8 (2017) 1811.

[85] K. Karimi, J.E. Boudreau, K. Fraser, H. Liu, J. Delanghe, J. Gauldie, Z. Xing, J.L. Bramson, Y. Wan, Enhanced antitumor immunity elicited by dendritic cell vaccines is a result of their ability to engage both CTL and ifnγ-producing NK cells, Mol. Ther. 16 (2008) 411–418.

[86] R.I. Fisher, E.R. Gaynor, S. Dahlberg, M.M. Oken, T.M. Grogan, E.M. Mize, J.H. Glick, C.A. Coltman, T.P. Miller, A phase III comparison of CHOP vs. m-BACOD vs. ProMACE-CytaBOM vs. MACOP-B in patients with intermediate- or high-grade non-Hodgkin\"s lymphoma: results of SWOG-8516 (Intergroup 0067), the National High-Priority Lymphoma Study, Annals of Oncology Official Journal of the European Society for Medical Oncology 5 (1994) S91–S95.

[87] C. Schmidt, The benefits of immunotherapy combinations, Nature (2017) 552.

[88] A. Showalter, A. Limaye, J. Oyer, R.Y. Igarashi, C. Kittipatarin, A.J. Copik, A.R. Khaled, Cytokines in immunogenic cell death: applications for cancer immunotherapy, Cytokine 97 (2017) 123–132.

[89] R.A. Lake, B. Robinson, Immunotherapy and chemotherapy–a practical partnership, Nat. Rev. Canc. 5 (2005) 397–405.

[90] L.A. Emens, G. Middleton, The interplay of immunotherapy and chemotherapy: harnessing potential synergies, Cancer immunology research 3 (2015) 436–443.

[91] P. Feugier, A review of rituximab, the first anti-CD20 monoclonal antibody used in the treatment of B non-Hodgkin's lymphomas, Future Oncol. 11 (2015) 1327–1342.